

A Local Approach to the Dynamics of Star Polymers

Marina Guenza, Michele Mormino, and Angelo Perico*

Centro di Studi Chimico-Fisici di Macromolecole Sintetiche e Naturali, CNR,
Corso Europa 30, 16132 Genova, Italy

Received March 15, 1991; Revised Manuscript Received June 7, 1991

ABSTRACT: The optimized Rouse-Zimm approach to the local dynamics of polymer solutions (ORZLD: Perico, A. *Acc. Chem. Res.* 1989, 22, 336) is extended to describe star polymers. A first-order model in the ORZLD hierarchy is defined for dilute Θ solutions, based on a freely rotating chain (FRC) description of semiflexible stars. The effects of the correlation at the star center and of the total or partial stretching of the arms due to segment concentration in the interior of the star are approximately taken into account. The partially stretched FRC star model is found in fairly good agreement with the available shrinking factor data on polystyrene stars as a function of the molecular weight. Strong effects are calculated for the slowing down of the correlation times for the bond relaxation in the interior of the star.

Introduction

On a local spatial scale, star polymers display very different monomer concentrations.¹⁻³ This concentration is as high as in the melt at the center but decreases to that of a dilute solution in the outer regions.³ In a long linear homopolymer, all the properties are uniform along the chain with the exception of end effects whose range becomes asymptotically irrelevant. For a star polymer of very long and equal arms regularly joined at the center, the local static and dynamic properties near the center and in the outer regions are strongly different.

These very peculiar properties were tested by many experimental techniques like viscosimetry, light scattering, and small-angle neutron scattering (SANS). Properties such as the radius of gyration, the hydrodynamics radius, static and dynamic structure factors, the intrinsic viscosity, and the Huggins coefficient were studied⁴⁻¹⁰ as a function of the total number of arms f in the star.

Static and dynamic structure factors are of particular interest as they give information on different length and time scales.

Local properties could be well discriminated by NMR relaxation times and NOE experiments especially on label nuclei or by fluorescence anisotropy on polymers with a fluorescent label.

One of the more outstanding features emerging from experimental data, Monte Carlo simulations, and renormalization group (RG) calculations is that in good solvents the shrinking factor g , the ratio of the mean-square radius of gyration of the star to that of the linear polymer at the same molecular weight, is close to the Gaussian ideal result of Zimm-Stockmayer,¹ thus showing a remarkable insensitivity to excluded volume.¹¹ Also the scaling prediction of Daoud and Cotton,³ $g \approx f^{-4/5}$ (large f) is almost indistinguishable from the $3f^{-1}$ (large f) Gaussian result, taking into account the inability for scaling to predict prefactors.^{4,11} On the contrary, in Θ solutions, despite the difficulties in locating the Θ point, the shrinking factor, evaluated experimentally or derived by simulations, RG theory, or scaling, tends to be always greater than the Gaussian value, this difference increasing with f .^{4,5,11} This deficiency of the Gaussian model for Θ stars could be due to ternary interactions whose probability increases with chain branching.¹¹

In this paper, simple star polymer models in Θ solvent are discussed with reference to the main experimental indications. These models are based on a freely rotating

chain picture with possible extensions to the rotational isomeric state (RIS) or other more detailed descriptions. Following Mansfield and Stockmayer¹² the proposed models are devised to describe the influence of the stiffness and of the correlation at the branch point on the solution properties in Θ conditions. But, according to the suggestions of Huber, Burchard, and co-workers,⁵ a rough model is introduced to take into account the stretching of the arms due to the concentration in the core of the star, getting ultimately the behavior of the blob model.³

The ORZLD (optimized Rouse-Zimm local dynamics) approach^{13,14} to the dynamics of polymer chains may be of great utility to study star polymers, as in this framework the local properties of these highly nonuniform objects can be easily approached for a wide hierarchy of polymer models. In this paper the ORZLD procedure is generalized to include the above models as a first approximation to the dynamics of dilute Θ solutions of star polymers. Results for the bond correlation times of the main local regions are presented and discussed. Recently an extension of the Gaussian Zimm model to deal with several polymer architectures including uniform stars was proposed.¹⁵ Viscoelastic and oscillatory flow birefringence properties were derived. This model may be considered as zero order in the optimized Rouse-Zimm hierarchy.¹³ Here we focus on local relaxation properties of semiflexible stars with internal concentration effects. Extensions to include explicitly binary or ternary interactions and more detailed polymer models are in progress.

Partially Stretched Freely Rotating Chain Arms for Star Polymers in the Θ State

Consider a star of f arms, each one with N bonds of length l , and a total number of beads n :

$$n = Nf + 1 \quad (1)$$

Each arm is a freely rotating chain (FRC) with a valence angle θ' for the first N' ($\leq N$) bonds and θ for the remaining $N - N'$ bonds with

$$p' = -\cos \theta' \quad (2)$$

$$p = -\cos \theta \quad (3)$$

the stiffness of the core and of the outer part of the star, respectively. (The symbol p for the stiffness of the FRC instead of the usual g is used to avoid confusion with the shrinking factor.)

The arms have equivalent correlations at the branch point

$$\langle \mathbf{l}_i \cdot \mathbf{l}_j \rangle / l^2 = \alpha_{ij} = \alpha \quad (4)$$

for any couple of arms i and j . Taking into account that the mean-square length of the vector

$$\mathbf{P} = \sum_{i=1}^f \mathbf{l}_i \quad (5)$$

must be positive definite

$$\langle P^2 \rangle = \sum_{i=1}^f \sum_{j=1}^f \langle \mathbf{l}_i \cdot \mathbf{l}_j \rangle / l^2 \geq 0 \quad (6)$$

it follows that¹²

$$-(f-1)^{-1} \leq \alpha \leq 1 \quad (7)$$

For $\alpha = -(f-1)^{-1}$ the star center has spherical symmetry. This symmetry is progressively lost as α increases. For $\alpha = 0$ (obtained also in the limit of large f) there is no correlation at the branch point, while in the limit $\alpha = 1$, all the first bonds of the star arms are superimposed, and the star takes the shape of a horse tail.

For this model the mean-square radius of gyration, $\langle S^2 \rangle_s$, can be calculated exactly (see Appendix A) as

$$\langle S^2 \rangle_s = l^2(f/n^2)[S_{\text{self}} + (f-1)S_{\text{cross}}] \quad (8)$$

with S_{self} and S_{cross} the contributions due to one or two arms, respectively

$$S_{\text{self}} = (N' + 1)^2 \langle S^2(N', p') \rangle_l / l^2 + (N - N' + 1)^2 \times \langle S^2(N - N', p) \rangle_l / l^2 + (N - N')F(N', p') + N'F(N - N', p) + 2p(p-1)^{-1}(p'-1)^{-1}G(N', p')G(N - N', p) \quad (9)$$

$$S_{\text{cross}} = NF(N', p') + N(N - N') \langle R^2(N', p') \rangle_l / l^2 + NF(N - N', p) + 2Np[(p')^{N'} - 1](p-1)^{-1} \times (p'-1)^{-1}G(N - N', p) - \alpha\{(N - N')[(p')^{N'} - 1](p'-1)^{-1} + p(p')^{N'-1}(p-1)G(N - N', p) + G(N', p')(p'-1)^{-1}\}^2 \quad (10)$$

where $\langle S^2(N, p) \rangle_l$ and $\langle R^2(N, p) \rangle_l$ are the mean-square radius of gyration and end-to-end distance for a freely rotating linear chain of N bonds and stiffness p , respectively, and

$$F(N, p) = (1+p)(1-p)^{-1}N(N+1)/2 - 2pN(1-p)^{-2} + 2p^2(1-p^N)(1-p)^{-3} \quad (11)$$

$$G(N, p) = (p^{N+1} - 1)(p-1)^{-1} - (N+1) \quad (12)$$

The star model here sketched is compared with a linear freely rotating chain of stiffness p , the same molecular weight or total number of beads n , and mean-square radius of gyration

$$\langle S^2 \rangle_l = (l^2/n)\{F(n, p) - (1+p)(n+1)(2n+1) \times (1-p)^{-1}/6 + p(n+1)(1-p)^{-2} - 2p^2[(1-p^n)/(n-p^n(1-p))](1-p)^{-4}\} \quad (13)$$

The measure of the contraction of the star, the shrinking factor g , is then defined as

$$g = \langle S^2 \rangle_s / \langle S^2 \rangle_l \quad (14)$$

The blob model takes into account the effect of segment

concentration in the interior of the star and finds that even in the Θ state the arm conformation is stretched, and, in the limit of large f and large N , $g \approx f^{-1/2}$. The scaling results are confirmed by a modified Flory approximation in both good and Θ solvents and are in qualitative agreement with RG calculations.¹¹ Assuming $N = N'$, eq 14 with eqs 8 and 13 gives in the limit of large N

$$\lim_{N \rightarrow \infty} g = \frac{(1+p')/(1-p')}{(1+p)/(1-p)}(3f-2)/f^2 \quad (15)$$

In the case $p = p' = 0$, the Gaussian result typical of the random-walk chain is recovered

$$g_{\text{rw}} = (3f-2)/f^2 \quad (16)$$

If eq 15 is constrained to reproduce the prediction of the blob model, $f^{-1/2}$, an estimate of the stretching of the arms is obtained as

$$\frac{(1+p')/(1-p')}{(1+p)/(1-p)} = cf^{3/2}/(3f-2) \quad (17)$$

with c a constant taking into account the prefactors not included in the scaling arguments of the blob theory. Note that in the modified Flory approximation the prefactor c for the scaling prediction in good solvents, $g = cf^{4/5}$, is found to be 1.94, while the Monte Carlo estimates are about $1.8 \div 1.9$.¹¹ In the Θ solvents there is not an estimation, but similar values are expected. Given the stiffness of the linear polymer, p , the molecular weight dependences of $\langle S^2 \rangle_s$ and g are then obtained, assuming $N = N'$, respectively, from eq 8 and eq 14 using eq 13.

Recent extensive experimental results⁴ for long-arm polyisoprene stars with branch point functionality f ranging from 3 to 56 under Θ conditions gave an exponent for the g dependence on f equal to -0.562 , a little bit lower than -0.5 predicted by the blob model but much larger than the Gaussian exponent -1.0 , $(3f-2)/f^2 \approx f^{-1}$. A similar behavior was found for polybutadiene stars.¹⁰ On the other hand, several authors^{5,8} found by light scattering and SANS a molecular weight dependent g for high enough functionality. They underline that, for $f \leq 6$ and high M , substantial agreement is found with the Gaussian g_{rw} factor, while, for larger f , g is greater but perhaps approaching again the Gaussian factor for higher M . This inference is confirmed by fitting the scattering function with a broken wormlike model (wormlike arms freely jointed at the branch point).⁶ A best fit in the region of wave vector $q < 0.4 \text{ nm}^{-1}$ is obtained, with Kuhn lengths of the broken wormlike model being higher, the smaller M is. This seems an evidence that only the portion of the arm in the interior of the star is stretched, while the outer portion behaves like linear chains. A similar indication emerges from the work of Lantman et al.⁷ on SANS studies of star block copolymers, although in good solvents, when the experiments probe the deuterated outer regions, dimensions are found to be identical with the free chain.

Thus, as suggested by Huber, Burchard, and others,^{5,6} another model can be considered with the first N' bonds in the star having an enhanced stiffness p' and the outer $N - N'$ bonds having the stiffness of the same linear chain in Θ conditions. This is a rough approximation to the arms with the stiffness continuously decreasing with the increasing of the distance from the star center and getting in the limit the free chain value. It is evident that in the limit $N \gg N' \gg 1$, this model from eqs 14, 8, and 13 recovers the Gaussian factor g_{rw} . The parameters N' and p' , characterizing the molecular weight dependence at con-

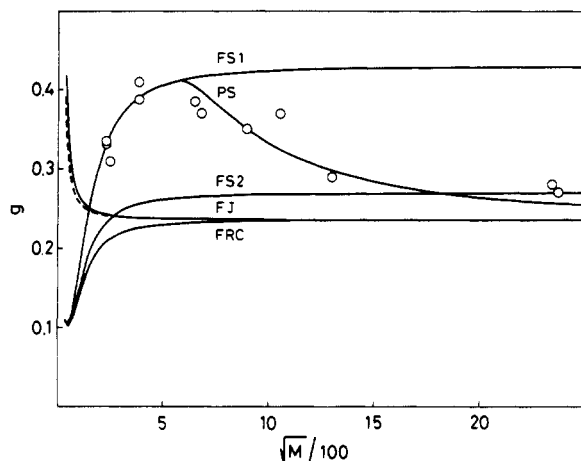


Figure 1. Shrinking factor g for polystyrene star at $f = 12$ as a function of the molecular weight. All the full curves have $\alpha = -(f-1)^{-1}$. FS1 and FS2: fully stretched arm models, respectively, at $p' = 0.87$ and $p' = 0.80$. PS: partially stretched arm model at $p' = 0.87$, $p = 0.77$, and $N' = 250$. FJ: freely jointed star model (the dashed curve has $\alpha = 0$). FRC: freely rotating star model at $p = 0.77$. Experimental data (O) are from refs 5, 8, and 9.

stant f , may be evaluated by careful fitting with experiments.

Similar results were obtained by a star model characterized by branches emerging from the surface of an impenetrable sphere describing the star core.¹⁶

It has to be stressed that this partially stretched arm star model with $\alpha = -(f-1)^{-1}$ is spherically symmetric. Therefore, it cannot display any umbrella shape as found by Ganazzoli et al.,¹⁷ taking explicitly into account the repulsive screened interactions arising from the intrinsic chain thickness as the origin of the stretching of the arms.

In Figure 1 the shrinking factor g , for $f = 12$ and $\alpha = -(f-1)^{-1}$, as a function of the molecular weight is reported for the fully and partially stretched FRC star models, for the FRC star model, and for the freely jointed star model ($N = N'$, $p = p' = 0$). Also reported are experimental results on polystyrene (PS) stars by different authors.^{5,8,9} Light scattering data of Huber et al.⁵ are not considered because they do not closely match SANS data for similar M and more recent data.⁸ Nevertheless, the considerations here reported do not qualitatively change using all the data. The value of $p = 0.77$ is obtained by fitting the linear FRC model to the experimental results for linear PS in Θ solvents.¹⁸ The value of $p' = 0.87$ is obtained by fitting eq 14, with eqs 8 and 13 and $N = N'$, to the data for the lower molecular weights, on the assumption that these short arms are totally stretched. Then $N' = 250$ is obtained by fitting all the data. The upper curve corresponds to a fully stretched model at $p' = 0.87$, and for $N' \rightarrow \infty$ gives the scaling result with $c = 1.5$, a reasonable value consistent with the discussion following eq 17. If the fully stretched model is constrained to reproduce the g values for the highest M , a much lower curve is obtained having $p' = 0.80$ and $c = 0.93$. Note that the fully stretched models cannot display any decrease of g with M . On the contrary a fairly good fit to the experimental data is obtained by the partially stretched model (curve PS in Figure 1).

Also reported are the curves for the freely jointed star model with correlation at the branch point $\alpha = -(f-1)^{-1}$ and without correlation, $\alpha = 0$. The comparison of these two curves shows a small effect indeed. In fact the contribution of α is appreciable mainly at small f and becomes in any case irrelevant at large M . The lower curve in Figure 1 corresponds to a FRC star with $p = 0.77$ and

$N = N'$, a case equivalent to the Mansfield-Stockmayer wormlike model.¹² As it is well-known, semiflexible star models give a shrinking ratio increasing asymptotically with M to the Gaussian limit and therefore cannot explain the experimental behavior.

ORZLD Approach to the Dynamics of Star Polymers: Bond Correlation Times

A review of the ORZLD approach was given elsewhere.¹³ Here, a few considerations are added to extend the treatment to the star architecture.

In a homogeneous star, the n beads, of equal friction coefficient ζ , are conventionally ordered as $i = 1$ for the star center and $i = 2, \dots, N+1$; $N+2, \dots, 2N+1$; ... for the bead sequence of the f arms. The bead coordinates evolve in time according to a linearized Langevin equation specified by a bond rate constant

$$\sigma = 3k_B T / l^2 \zeta \quad (18)$$

a static bond correlation matrix

$$\mathbf{U}_{ij}^{-1} = \langle \mathbf{l}_i \mathbf{l}_j \rangle / l^2 \quad (19)$$

and the adimensional mean inverse distances $\langle l/R_{ij} \rangle$. In the Gaussian approximation, this average is in turn given in terms of \mathbf{U}^{-1} :

$$\langle l/R_{ij} \rangle = l(6/\pi)^{1/2} (\langle R_{ij}^2 \rangle)^{-1/2} \quad (20)$$

and

$$\langle R_{ij}^2 \rangle = l^2 \sum_{r,s=i+1}^j \mathbf{U}_{rs}^{-1} \quad j > i \quad (21)$$

Given \mathbf{U}^{-1} and $\langle l/R_{ij} \rangle$, the structural matrix \mathbf{A} and the hydrodynamic interaction matrix \mathbf{H} are calculated as

$$\mathbf{A} = \mathbf{M}^T \begin{pmatrix} 0 & 0 \\ 0 & \mathbf{U} \end{pmatrix} \mathbf{M} \quad (22)$$

$$\mathbf{H}_{ij} = \delta_{ij} + \zeta_r \langle l/R_{ij} \rangle (1 - \delta_{ij}) \quad (23)$$

where \mathbf{U} is the inverse of \mathbf{U}^{-1} and

$$\zeta_r = \zeta / 6\pi\eta_0 l \quad (24)$$

is the hydrodynamic interaction strength (0.25 in Θ solutions). The bead-to-bond vector transformation matrix \mathbf{M} , which is a function of the architecture of the polymer, is defined as

$$\begin{aligned} \mathbf{M}_{1i} &= n^{-1} & i &= 1, \dots, n \\ \mathbf{M}_{ii} &= 1 & i &= 2, \dots, n \\ \mathbf{M}_{i+1,i} &= -1 & i &= 2, \dots, N; N+2, \dots, 2N; \dots \\ & & & (f-1)N+2 \dots fN \\ \mathbf{M}_{i1} &= -1 & i &= 2, N+2, 2N+2, \dots, (f-1)N+2 \\ \mathbf{M}_{ij} &= 0 & \text{otherwise} \end{aligned} \quad (25)$$

Static and dynamic quantities are then obtained in terms of the $n-1$ nonzero eigenvalues λ_a , eigenvectors $\{\mathbf{Q}_{ia}\}$, and mean-square lengths of the modes $l^2 \mu_a^{-1}$, diagonalizing the product matrix $\mathbf{H}\mathbf{A}$ in the Langevin ORZLD equation. As a typical local property, let us consider the adimensional bond correlation times τ^i for the second-order bond time correlation function (TCF), $P_2^i(t)$:

$$\tau^i = \int_0^\infty P_2^i(\sigma t) d\sigma t \quad (26)$$

In the ORZLD approach $P_2^i(t)$ is derived exactly as

$$P_2^i(t) = 1 - 3\{x^2 - x^3(\pi/2)[1 - (2/\pi) \arctan x]\} \quad (27)$$

where

$$x = [1 - (M_1^i(t))^2]^{1/2} / M_1^i(t) \quad (28)$$

and

$$M_1^i(t) = \sum_{a=1}^{n-1} (Q_{ia} - Q_{i-1,a})^2 \mu_a^{-1} \exp(-\sigma \lambda_a t) \quad (29)$$

For a homogeneous star the τ^i are equivalent on each arm. Therefore τ^i for an arm of length N will be studied and compared with the τ^i for a linear chain of the same length. Clearly, a full hierarchy of dynamic models, characterized by specific U^{-1} (and $\langle l/R_{ij} \rangle$), may be considered. Short-range interactions can be better included using rotational isomeric state (RIS) type models.^{13,19} More refined models of the stretching of the star arms due to bead concentration can be considered, taking into account long-range binary and ternary interactions in Θ and good solvents.^{20,21}

As a first-order approximation to the dynamics of star polymers in Θ solutions, the star with partially stretched freely rotating arms of the previous section, in a Gaussian approximation for $\langle l/R_{ij} \rangle$, is discussed. This model should take into account two physical features characterizing the local relaxation times of a star arm in comparison to a linear chain of the same length of the arm. The first and most important is the shift of the center of mass toward one end of the arm due to the topological connection at the center of the f arm star. This effect does exist even in a simple Gaussian or semiflexible star. The second feature is the partial stretching of the arm due to the segment concentration in the star core. It was shown in the first section that a moderate increasing of the local stiffness in the core affects long-range static properties as the g dependence on molecular weight. It is expected that this local increase of stiffness causes an additional effect on the local relaxation times.

In this first-order model, the matrix U^{-1} is

$$U^{-1} = \begin{bmatrix} \mathbf{D} & \mathbf{S} & \mathbf{S} \dots \mathbf{S} & \mathbf{S} \\ \mathbf{S}^T & \mathbf{D} & \mathbf{S} \dots \mathbf{S} & \mathbf{S} \\ \dots & \dots & \dots & \dots \\ \dots & \dots & \mathbf{D} & \mathbf{S} \\ \dots & \dots & \mathbf{S}^T & \mathbf{D} \end{bmatrix} \quad (30)$$

The matrix is of order fN , and \mathbf{D} and \mathbf{S} are submatrices of order N relative to the bond correlations on the same arm or between two different arms, respectively:

$$\mathbf{D} = \begin{pmatrix} \mathbf{D}_1 & \mathbf{D}_2 \\ \mathbf{D}_2^T & \mathbf{D}_3 \end{pmatrix} \quad \mathbf{S} = \begin{pmatrix} \mathbf{S}_1 & \mathbf{S}_2 \\ \mathbf{S}_2^T & \mathbf{S}_3 \end{pmatrix} \quad (31)$$

\mathbf{D}_1 and \mathbf{S}_1 are square matrices of order N' describing bond correlations between the stretched portion of a single arm or a couple of arms, respectively. Similarly, \mathbf{D}_3 and \mathbf{S}_3 are square matrices of order $N - N'$ relative to the nonstretched portions, while \mathbf{D}_2 and \mathbf{S}_2 are rectangular matrices $N'(N - N')$ coupling stretched and nonstretched portions. Using the definitions in the previous section, the elements of these matrices are

$$(\mathbf{D}_1)_{ij} = (p')^{i-j}; \quad (\mathbf{D}_2)_{ij} = (p')^{N'-i} p^j; \quad (\mathbf{D}_3)_{ij} = p^{i-j} \quad (32)$$

$$(\mathbf{S}_1)_{ij} = \alpha (p')^{i+j-2}; \quad (\mathbf{S}_2)_{ij} = \alpha (p')^{N'+i-2} p^j; \quad (\mathbf{S}_3)_{ij} = \alpha (p')^{2N'-2} p^{i+j} \quad (33)$$

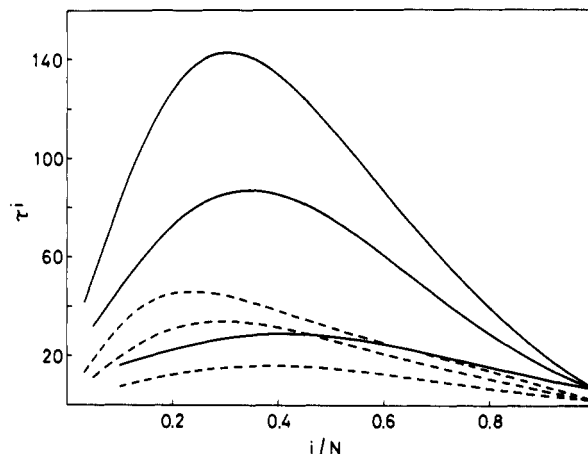


Figure 2. Bond correlation times τ^i as a function of the relative distance to the star center i/N for an arm of length N ; $f = 12$ and $\alpha = 0$. Freely rotating stars with $p = 0.87$ (full curves) and $p = 0.77$ (dashed curves); $N = 10, 20$, and 30 (from bottom to top).

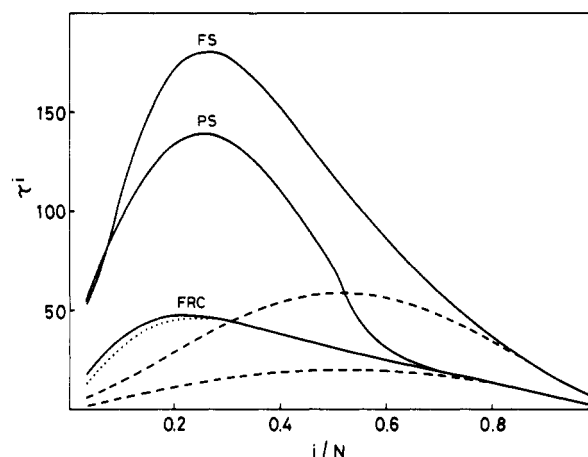


Figure 3. Bond correlation time τ^i as a function of i/N for an arm of length $N = 30$, $f = 12$, and $\alpha = -(f - 1)^{-1}$. FS: fully stretched arm model with $p' = 0.87$. PS: partially stretched arm model with $p = 0.77$, $p' = 0.87$, and $N' = N/2$. FRC: freely rotating chain star model at $p = 0.77$. The dotted curve has $\alpha = 0$. Linear freely rotating chain of length $N = 30$ (dashed curves): upper curve, $p = 0.87$; lower curve, $p = 0.77$.

Note that, in the limit $N = N'$ and $p = p'$, the matrices \mathbf{D} and \mathbf{S} reduce to \mathbf{D}_1 and \mathbf{S}_1 , and U^{-1} describes the freely rotating star of stiffness p with a correlation α at the center.

It has been shown^{22,23} quantitatively that for a linear polymer in Θ conditions the ORZ correlation time τ^i increases with stiffness from the Gaussian value to the limit of a rod. In this last case τ^i becomes independent of i and equal to the rotational correlation time of the rod. For Gaussian and semiflexible chains, τ^i is a bell-shaped symmetric function of i , increasing with the bead number N toward a limit curve. In an ideal Gaussian or semiflexible (FRC) star the symmetry of τ^i around the middle of the arm is lost due to the presence of the f arms.

In Figure 2 the distortion of the symmetric curve for τ^i with i/N is shown for FRC stars of stiffness $p = 0.77$ and 0.87 . Again the curves increase with p and with N as in the linear case, but the maximum shifts from the center of the arm $i = N/2$ toward the center of the star $i = 1$: the stiffer the arm, the less the shift; the longer the arm, the larger the shift. On the contrary, for the $i/N \rightarrow 1$ limit the star curve sticks to the linear chain curve (see Figure 3).

This slowing down of the correlation times at the star center strongly increases with the number of arms f . It

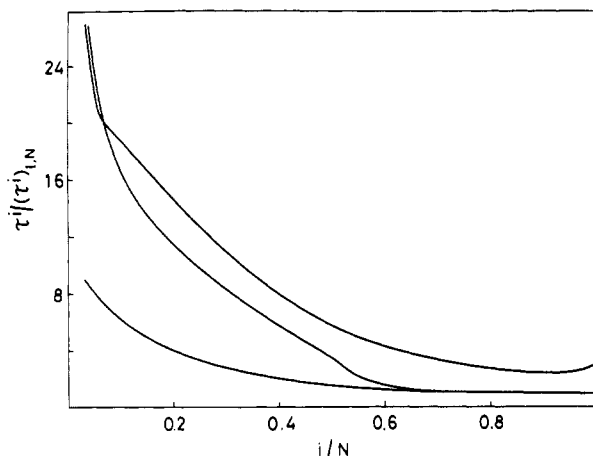


Figure 4. Slowing ratio for the bond correlation time of the star τ^i relative to that of a linear FRC chain of length N (arm length) $(\tau^i)_{L,N}$, as a function of i/N ; $N = 30$; $\alpha = -(f-1)^{-1}$; $f = 12$. Fully stretched arm model (upper curve): $p' = 0.87$. Partially stretched arm model (medium curve): $p' = 0.87$, $p = 0.77$; $N' = N/2$. FRC star model (lower curve): $p = 0.77$.

has to be stressed that this effect is due to the topology of the star, affecting the center of mass position, and not to the correlation α at the star center, which is a minor effect. As a matter of fact, the curves of Figure 2 are calculated at $\alpha = 0$. Nevertheless, a negative correlation at the center, $\alpha = -(f-1)^{-1}$, increasing the symmetry of the star at the center, increases the slowing down of the correlation times at the star center, $i/N \ll 1$. This can be appreciated in Figure 3 where the τ^i at $p = 0.77$ are reported for $\alpha = 0$ and $\alpha = -(f-1)^{-1}$.

Figure 3 reports the correlation times τ^i as a function of i/N for the main models studied in this paper: the pure FRC linear chains (of length N) and stars at $p = 0.77$ and $p = 0.87$ and the partially stretched stars with $p = 0.77$ and $p' = 0.88$. Here for the partially stretched star model $N' = N/2$ was chosen. As a matter of fact, the exact calculation of the ORZLD models can be performed only up to 360 for n . This in turn implies an upper limit in N around 30, much lower than the values of N' estimated in section II. Nevertheless, the chain with $N' = N/2$ catches the essential features of the τ^i behavior. Note that the fully stretched model is simply a FRC star model with an enhanced stiffness parameter. In the limit $i/N \rightarrow 1$ the fully stretched models give correlation times coincident with those of a free arm of the same stiffness. The partially stretched star, in this same limit, displays a decrease of τ^i toward the τ^i of a free arm with stiffness p . On the left-hand side of the figure the strongest slowing down is observed for the fully stretched model. A slightly lower slowing down is observed for the partially stretched model in the range $i \ll N'$.

Globally the topological slowing down of the correlation times for the partially stretched arm model is intermediate between the fully stretched arm model and the FRC model at p . The fully and partially stretched models display a significantly larger slowing down than the simple FRC star.

The ratio of τ^i in the star to the τ^i in the linear chain of length equal to the arm length $(\tau^i)_{L,N}$ is assumed as an index of the topological slowing down of the bond correlation time. This ratio is reported in Figure 4 for the fully stretched arm model ($p' = 0.87$), for the FRC arm model ($p = 0.77$), and for the partially stretched star model ($p = 0.77$, $p' = 0.87$, and $N' = N/2$). The denominator $(\tau^i)_{L,N}$ is calculated for a linear FRC of stiffness $p = 0.77$ and length $N = 30$.

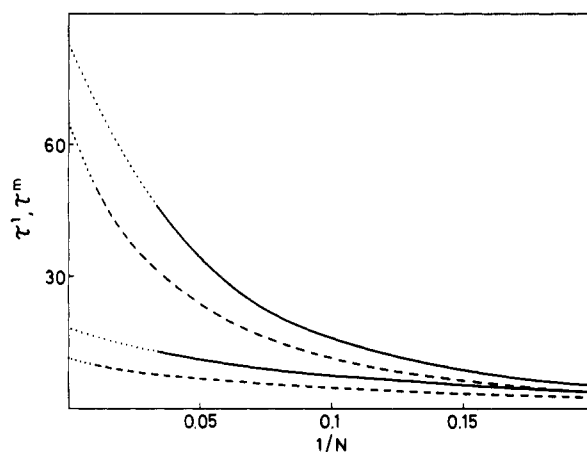


Figure 5. Correlation times τ^i (lower curves) and τ^m as a function of N^{-1} for a FRC star with $p = 0.77$. Dotted curves: extrapolation to $N \rightarrow \infty$. Full curves: $f = 12$. Dashed curves: $f = 3$.

The slowing ratio is in any case very large at the star center and becomes much lower in the outer region of the star. In the limit $i \rightarrow N$ it takes the value 1 for the FRC and the partially stretched model. For the fully stretched model, at large i/N , a value is obtained correlated with the stiffness induced by the segment concentration effect. These results for partially stretched stars are in a fairly good agreement with RG considerations on many-arm stars and with oscillatory flow birefringence experiments showing strong slowing down of the internal modes while the modes of outer regions remain compatible with those of the linear polymer.²⁴

The discussion on local relaxation times is here confined to short arms. As a matter of fact, a maximum arm length of $N = 30$ could be reached for $f = 12$ using the exact ORZLD procedure while reliable approximate treatments are under study for large N . Nevertheless, some general predictions can be stressed about the long-arm limit. In Figures 2–4 the abscissas i/N are used to normalize the arm length and compare curves at different N . For linear chains the minimum relaxation time τ^1 and the maximum τ^m located in the middle of the chain asymptotically increase with N to constant values. The ratio τ^m/τ^1 runs from 10 at $N = 30$ to 17 at $N = 100$ for $p = 0.77$ and from 10 to 23 for $p = 0.87$. Note that a RIS model for linear PS gave similar results.²³ This indicates a model independence of the behavior for local relaxation times as calculated for flexible linear polymers by ORZLD. In addition, these ORZLD results for linear chains were confirmed by anisotropy relaxation experiments on polypeptides²⁵ and by NMR relaxation experiments on ¹³C located on the backbone and on the lateral chains of synthetic polymers.²⁶ Also for stars it is expected that τ^1 and τ^m , with τ^m the maximum relaxation time in the chain, increasing asymptotically with N .

An estimation of this asymptotic enhancement of the slowing down with N for semiflexible stars is obtained by plotting τ^1 and τ^m for a FRC star with $p = 0.77$ against N^{-1} . In addition to the results for $f = 12$, results for $f = 3$ are reported as the extrapolation is here more reliable. Figure 5 shows that all the relaxation times increase to finite values for $N \rightarrow \infty$, with the dependence on N being more relevant for τ^m than for τ^1 . Note that the limiting values are longer, the larger f is.

In conclusion, Figure 3 is expected to give a qualitative description (although quantitatively changing increasing N) of the local relaxations in PS star polymers in Θ conditions. Given a specific $N = \bar{N}$, the real relaxation curve is expected between the curves FS ($p = 0.87$ at N

= \bar{N}) and FRC ($p = 0.77$, $N = \bar{N}$), although not necessarily stuck to the curve PS obtained by the rough partially stretched model. However, the real curve should stick to FS to the left and to FRC to the right.

Notwithstanding the roughness of the models here discussed, it appears clear that accurate measurements of local relaxation times can discriminate between models, thus giving a better insight to the star physical behavior.

Conclusions

A local approach to the dynamics of star polymers has been presented and discussed. This approach is based on the optimized Rouse-Zimm approximation to polymer dynamics. A first-order model is proposed for Θ solutions, which takes roughly into account the stretching in the star arms, caused by the high concentration in the star core. The model has semiflexible arms (described as a freely rotating chain) with correlation at the star center. The basic stiffness of the star is derived from that of the equivalent linear chain, while the stretching is determined by comparison to the experimental molecular weight dependence of the shrinking factor g . The stretching of the arms may be extended to the whole arm length, consistent with the scaling hypothesis, or limited to a core region, eventually recovering in the limit of very long arms the Gaussian behavior. The partially stretched arm model seems to describe very well the peculiar molecular weight dependence of g found by many authors for PS in Θ solutions.

The bond correlation times for the fully and partially stretched models together with the FRC star model are calculated and analyzed. Very large effects are predicted for the slowing down of these relaxation processes, particularly for the inner regions in the star. In addition, fully and partially stretched arm models and simple semiflexible models present largely different behaviors. Therefore, the possibility of using local dynamics measurements to get information on the physical processes affecting the star conformation and dynamics exists.

Large effects are expected also for the viscosity and hydrodynamic shrinking factors and for the static and dynamic structure factors. These effects are under current investigation. The rough models discussed here are only a first-order approximation to a full hierarchy of models amenable to calculation in the ORZLD approach. Work is in progress to explicitly include binary and ternary interactions together with more detailed polymer models (RIS models).

Appendix A

The mean-square radius of gyration

$$\langle S^2 \rangle = (1/2n^2) \sum_{i,j=1}^n \langle R_{ij}^2 \rangle \quad (A1)$$

for a star is first separated into two terms, S_{self} and S_{cross} , considering the i and j indexes on the same or on different arms, respectively:

$$\langle S^2 \rangle_s = l^2 f / n^2 [S_{\text{self}} + (f-1)S_{\text{cross}}] \quad (A2)$$

In both cases, $\langle R_{ij}^2 \rangle$, the mean-square distance between i and j , can be written in terms of the distances from the star center:

$$\langle R_{ij}^2 \rangle = \langle R_{1i}^2 \rangle + \langle R_{1j}^2 \rangle - 2\langle \mathbf{R}_{1i} \cdot \mathbf{R}_{1j} \rangle \quad (A3)$$

When eq A3 is introduced into $\langle S^2 \rangle$, we get

$$S_{\text{self}} = N \sum_{i=1}^N \langle R_{1i}^2 \rangle / l^2 - \sum_{i,j=1}^N \langle \mathbf{R}_{1i} \cdot \mathbf{R}_{1j} \rangle / l^2 \quad (A4)$$

$$S_{\text{cross}} = N \sum_{i=1}^N \langle R_{1i}^2 \rangle / l^2 - \sum_{\substack{i,j=1 \\ \text{different} \\ \text{arms}}}^N \langle \mathbf{R}_{1i} \cdot \mathbf{R}_{1j} \rangle / l^2 \quad (A5)$$

In the partially stretched model each contribution in eqs A4 and A5 is split in stretched and nonstretched parts that can be calculated by introducing the bond vectors $\{\mathbf{l}_a\}$.

The calculation of $\langle R_{1i}^2 \rangle$ is broken into two parts

$i \leq N' + 1$

$$\langle R_{1i}^2 \rangle = \sum_{a=1}^{i-1} \sum_{b=1}^{i-1} \langle \mathbf{l}_a \cdot \mathbf{l}_b \rangle \quad (A6)$$

$i > N' + 1$

$$\langle R_{1i}^2 \rangle = \sum_{a=1}^{N'} \sum_{b=1}^{N'} \langle \mathbf{l}_a \cdot \mathbf{l}_b \rangle + \sum_{a=N'+1}^{i-1} \sum_{b=N'+1}^{i-1} \langle \mathbf{l}_a \cdot \mathbf{l}_b \rangle + 2 \sum_{a=1}^{N'} \sum_{b=N'+1}^{i-1} \langle \mathbf{l}_a \cdot \mathbf{l}_b \rangle \quad (A7)$$

The calculation of $\langle \mathbf{R}_{1i} \cdot \mathbf{R}_{1j} \rangle$ gives in the case of i and j on the same arm

$i, j \leq N' + 1$

$$\langle \mathbf{R}_{1i} \cdot \mathbf{R}_{1j} \rangle = \sum_{a=1}^{i-1} \sum_{b=1}^{j-1} \langle \mathbf{l}_a \cdot \mathbf{l}_b \rangle \quad (A8)$$

$i, j > N' + 1$

$$\langle \mathbf{R}_{1i} \cdot \mathbf{R}_{1j} \rangle = \sum_{a=1}^{N'} \sum_{b=1}^{N'} \langle \mathbf{l}_a \cdot \mathbf{l}_b \rangle + \sum_{a=1}^{N'} \sum_{b=N'+1}^{j-1} \langle \mathbf{l}_a \cdot \mathbf{l}_b \rangle + \sum_{a=N'+1}^{i-1} \sum_{b=1}^{N'} \langle \mathbf{l}_a \cdot \mathbf{l}_b \rangle + \sum_{a=N'+1}^{i-1} \sum_{b=N'+1}^{j-1} \langle \mathbf{l}_a \cdot \mathbf{l}_b \rangle \quad (A9)$$

$i \leq N' + 1; j > N' + 1$

$$\langle \mathbf{R}_{1i} \cdot \mathbf{R}_{1j} \rangle = \sum_{a=1}^{i-1} \sum_{b=1}^{N'} \langle \mathbf{l}_a \cdot \mathbf{l}_b \rangle + \sum_{a=1}^{i-1} \sum_{b=N'+1}^{j-1} \langle \mathbf{l}_a \cdot \mathbf{l}_b \rangle \quad (A10)$$

In the case of two different arms, the equations are formally identical with eqs A8–A10, with the \mathbf{l}_a and \mathbf{l}_b referring to different arms. The projection of \mathbf{l}_b on \mathbf{l}_a is calculated by the standard procedure developed for FRC. In the case of different arms, a continuous chain of length $a + b + 1$, correlated at the star center with a stiffness parameter $-\alpha$, is assumed. The remaining part of the calculation uses again and again the sums of geometric progressions to get the final results of eqs 9 and 10.

References and Notes

- (1) Zimm, B. H.; Stockmayer, W. H. *J. Chem. Phys.* **1949**, *17*, 1301.
- (2) Yamakawa, H. *Modern Theory of Polymer Solutions*; Harper & Row: New York, 1971.
- (3) Daoud, M.; Cotton, J. P. *J. Phys. (Paris)* **1982**, *43*, 531.
- (4) Bauer, B. J.; Fetters, L. J.; Graessley, W. W.; Hadjichristidis, N.; Quack, G. F. *Macromolecules* **1989**, *22*, 2337.
- (5) Huber, K.; Burchard, W.; Bantle, S.; Fetters, L. J. *Polymer* **1987**, *28*, 1990.

- (6) Huber, K.; Burchard, W. *Macromolecules* **1989**, *22*, 3332.
- (7) Lantman, C. W.; MacKnight, W. J.; Rennie, A. R.; Tassin, J. F.; Monnerie, L.; Fetters, L. J. *Macromolecules* **1990**, *23*, 836.
- (8) Khasat, N.; Pennisi, R. W.; Hadjichristidis, N.; Fetters, L. J. *Macromolecules* **1988**, *21*, 1100.
- (9) Roovers, J.; Hadjichristidis, N.; Fetters, L. J. *Macromolecules* **1983**, *16*, 214.
- (10) Roovers, J.; Toporowski, P.; Martin, J. *Macromolecules* **1989**, *22*, 1897.
- (11) Douglas, J. F.; Roovers, J.; Freed, K. F. *Macromolecules* **1990**, *23*, 4168.
- (12) Mansfield, M. L.; Stockmayer, W. H. *Macromolecules* **1980**, *13*, 1713.
- (13) Perico, A. *Acc. Chem. Res.* **1989**, *22*, 336.
- (14) Perico, A.; Guenza, M. *J. Chem. Phys.* **1985**, *83*, 3103.
- (15) Sammler, R. L.; Schrag, J. L. *Macromolecules* **1988**, *21*, 1132.
- (16) Boothroyd, A. T.; Ball, R. C. *Macromolecules* **1990**, *23*, 1729.
- (17) Ganazzoli, F.; Fontelos, M. A.; Allegra, G. *Polymer* **1991**, *32*, 170.
- (18) Huber, K.; Burchard, W.; Bantle, S. *Polymer* **1987**, *28*, 863.
- (19) Mattice, W. L. *Macromolecules* **1975**, *8*, 644.
- (20) Miyake, A.; Freed, K. F. *Macromolecules* **1983**, *16*, 1228.
- (21) Allegra, G.; Ganazzoli, F. *Adv. Chem. Phys.* **1989**, *75*, 265.
- (22) Perico, A.; Guenza, M. *J. Chem. Phys.* **1986**, *84*, 510.
- (23) Perico, A. *J. Chem. Phys.* **1988**, *88*, 3996.
- (24) Douglas, J. F.; Freed, K. F. *Macromolecules* **1985**, *18*, 2445.
- (25) Hu, Y.; Macinnis, J. M.; Cherayil, B. J.; Fleming, G. R.; Freed, K. F.; Perico, A. *J. Chem. Phys.* **1990**, *93*, 822.
- (26) Perico, A.; Altomare, A.; Catalano, D.; Colombani, M.; Veracini, C. A. *Macromolecules* **1990**, *23*, 4912.

Registry No. PS, 9003-53-6.